The American Association of Petroleum Geologists Bulletin
V. 76, No. 2 (February 1992), P. 191-198, 8 Figs., 1 Table

Relationship of Porosity and Permeability to Various Parameters Derived from Mercury Injection-Capillary Pressure Curves for Sandstone[1]

Edward D. Pittman[2]

ABSTRACT

Pore aperture size estimated from mercury injection tests has been used to evaluate seals for traps and to explain the locations of stratigraphic hydrocarbon accumulations. However, mercury injection tests are expensive and therefore not abundant. This paper develops empirical equations for estimating certain pore aperture size parameters from routine core analysis. The relationship of porosity, uncorrected air permeability, and various parameters derived from mercury injection–capillary pressure curves was established using multiple regression on a database of 202 samples of sandstone from 14 formations that range in age from Ordovician to Tertiary. These sandstone formations vary in composition and texture.

A series of empirically derived equations also permits the calculation of pore aperture radii corresponding to mercury saturation values that range from 10 to 75% in increments of five. This makes it possible to construct a calculated pore aperture radius distribution curve using porosity and permeability from core analysis.

INTRODUCTION

Reservoir engineers and petrophysicists are interested in how permeability and porosity relate to pore aperture size and pore aperture size distribution, primarily so they can estimate permeability. Exploration geologists have been interested in using pore aperture size derived from mercury injection data to evaluate the sealing capacity of cap rocks (e.g., Smith, 1966; Berg, 1975). In a water-saturated rock, hydrocarbon migration and entrapment result from the opposing interplay of buoyancy pressure and capillary pressure. Following expulsion from a source rock, hydrocarbons migrate through carrier beds when a hydrocarbon filament has been established through the pores of the rock. If one can determine the pressure required to establish a connected hydrocarbon filament through the largest interconnected water-saturated pore throats, one can calculate the vertical hydrocarbon column required to migrate hydrocarbons (Schowalter, 1979). This displacement pressure is important to hydrocarbon migration and entrapment .

The pore aperture size that corresponds to displacement pressure can be determined from a mercury injection test. However, often, one may want to know this information when mercury injection tests are unavailable because of cost considerations, lack of core, or insufficient core material (e.g., small chips or thin slabs) to permit sampling. Therefore, a readily available estimation of displacement pressure, from other data such as porosity and permeability, would be helpful.

Another parameter of interest is the pore aperture that corresponds to the apex of a hyperbola on a log-log mercury injection plot. This parameter has the potential for delineating stratigraphic traps in the same manner as the pore aperture corresponding to the 35th percentile of a cumulative mercury saturation curve, which was developed by H. D. Winland, Amoco Production Company.

The purpose of this paper is to (1) review previous efforts to relate permeability, porosity, and mercury injection–capillary pressure data; (2) present empirical relationships among porosity, uncorrected air permeability, and the pore aperture size that corresponds to the displacement pressure and the apex of a hyperbola on a log-log mercury injection plot; and (3) present empirically derived equations that permit construction of a pore aperture radius distribution curve using porosity and permeability data.

[1]Manuscript received May 8, 1990; revised copy received May 29, 1991; final acceptance July 22, 1991.

[2]Department of Geosciences, University of Tulsa, Tulsa, Oklahoma 74104.

The statistical analyses were done while the author was employed by Amoco Production Company using data in the Research Center files. Unpublished work by H. D. Winland, Amoco Production Company, provided the inspiration for this paper. One hundred-three of the 202 samples were from the Winland sample suite. I thank M. O. Traugott, D. R. Spain, and J. B. Thomas for their thoughtful and helpful reviews of the manuscript.

PREVIOUS WORK

Washburn (1921) first suggested the use of mercury injection as a laboratory method for determining the pore aperture size distribution in porous rocks. The Washburn equation can be expressed as

$$P_c = -2\gamma\cos\Theta/r \qquad (1)$$

where P_c = capillary pressure (dynes/cm^2), γ = surface tension of Hg (480 dynes/cm), Θ = contact angle of mercury in air (140°), and r = radius of pore aperture for a cylindrical pore. Thus, $r(\mu m) = 107/P_c(psia)$.

Van Brakel et al. (1981) discussed some of the problems of mercury porosimetry. One source of error in measuring rock porosity is that the pores are not necessarily cylindrical. Purcell (1949) was instrumental in developing mercury injection techniques, and equation 1 has been the basis of further work by many authors. Capillary pressure versus mercury saturation commonly is plotted on arithmetic or semilog plots (Figure 1), although the saturation scale sometimes is reversed so that it increases from right to left.

Entry pressure, displacement pressure, and threshold pressure are terms referring to the initial part of the mercury injection curve. The entry pressure on a mercury injection–capillary pressure plot is the point on the curve where the mercury first enters the pores of the rock. This point is indicative of the largest pore aperture size (Robinson, 1966). This parameter often is vague and difficult to determine because the sample size and surface irregularities of the rock relative to pore geometry create a boundary condition that affects the low-mercury saturation part of the curve. Schowalter (1979) recognized this problem and pointed out that the important aspect for evaluating seals for traps is to determine the pressure required to form a connecting filament of nonwetting fluid through the largest connected pore apertures of the rock. He measured this pressure by making electrical conductivity readings during mercury injection and found the mercury saturation ranged from 4.5 to 17%. Schowalter (1979) wanted a pragmatic approach to use on existing mercury injection data where electrical conductivity measurements were not available. Therefore, he defined the term displacement pressure as the pressure at 10% mercury saturation, for use in evaluation of hydrocarbon entrapment. Katz and Thompson (1986, 1987) defined threshold pressure as the pressure at which mercury forms a connected pathway across the sample. Katz and Thompson (1987) indicated that the measured threshold pressure corresponded graphically to the inflection point on a mercury injection plot. On Figure 1, this is where the mercury injection curve becomes convex upward.

Wood's metal, an alloy of bismuth that contains lead, tin, and cadmium and has a melting point of 70°C, has been used by various workers as a nonwetting medium for injection into pores of rocks. Dullien and Dhawan (1975) showed that injecting mercury and Wood's metal yielded similar injection curves. Molten Wood's metal can be cooled and crystallized at any desired injection pressure. One can evaluate the nature of the pore geometry occupied by Wood's metal using various techniques. Dullien and co-workers (e.g., Dullien and Dhawan, 1974) have used photographic methods employing quantitative stereology of Wood's metal to characterize pores, which consist of a series of bulges and necks. Dullien (1981) has compared pore size distributions derived from quantitative stereology and mercury porosimetry. The mercury injection technique indicates a greater quantity of small pores than does the quantitative stereology technique.

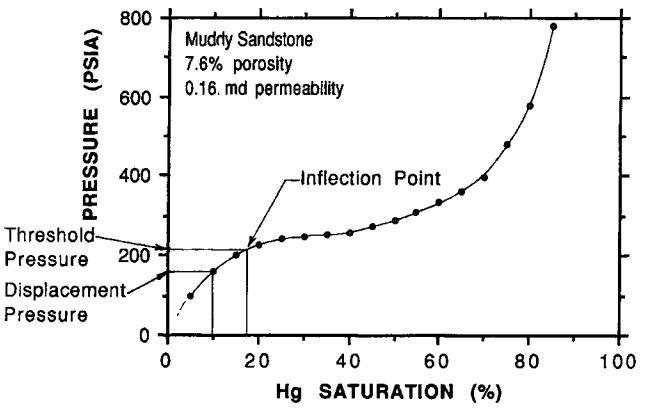

Figure 1—Presentation of mercury injection–capillary pressure data. Often this is presented as a semilog plot. The threshold pressure, as defined graphically by Katz and Thompson (1987), corresponds to the inflection point at which the curve becomes convex upward. The displacement pressure (P_d) was defined by Schowalter (1979) as the pressure at a mercury saturation of 10%.

Swanson (1977) established the position on the mercury injection curve that represents a continuous, well-interconnected pore system through the rock. He used a porosimeter with a heating coil and molten Wood's metal to illustrate visually the distribution of the nonwetting phase at various pressures. After having been injected at a low pressure, the cooled and crystallized Wood's metal had a spotty distribution in the rock. With increasing injection pressure, the nonwetting phase entered smaller pore apertures and the volume of the Wood's metal increased. Eventually, an injection pressure was reached whereby the Wood's metal occupied pore sizes that effectively interconnected the total major pore system that dominates fluid flow. Swanson (1977, p. 2498) noted that at this point, "the mercury saturation expressed as percent of bulk volume is indicative of that portion of the space effectively contributing to fluid flow." Swanson (1977) determined that on a mercury injection curve, this point corre-

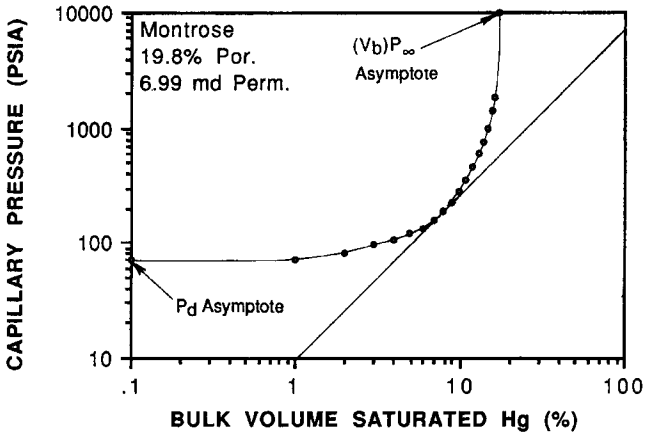

Figure 2—A log-log hyperbolic plot of mercury injection data following Thomeer (1960) and Swanson (1981). Thomeer used the values of the asymptotes in his mathematical description. The 45°-line is tangent to the hyperbola at the apex. Some mercury curves have no apex.

sponded to the apex of the hyperbola of a log-log plot. In Figure 2, the 45°-line is tangent to the hyperbola at the apex.

Thomeer (1960) developed a mathematical description of capillary pressure and mercury saturation, and first plotted mercury injection data as a log-log plot. This plot yields a curve that approximates a hyperbola (Figure 2). The location of the hyperbola with respect to the x and y axes is defined by the position of the two asymptotes. Thomeer called these the extrapolated displacement pressure (P_d on the y axis) and the bulk volume occupied by mercury at infinite pressure ($[V_b]P_\infty$ on the x axis). The shape of the hyperbola is related to pore geometry, which leads to Thomeer's pore geometrical factor (G). G is based on the possibility of a family of hyperbolic curves having G values from zero to 10, with low values constituting larger and better-sorted pore apertures and hence indicating better reservoir characteristics. Not all curves, however, are hyperbolic and suitable for assignment of G values. Thomeer (1960) showed graphically that a relationship exists among air permeability, $(V_b)P_\infty/P_d$, and G, and that pore geometry affects permeability and mercury injection.

Swanson (1981) developed the following relationship based on 319 clean sandstone and carbonate samples:

$$K_{air} = 339(S_{HG}/P_c)_{apex}^{1.691} \quad (2)$$

where K_{air} is air permeability (md), S_{HG} is the bulk volume mercury saturation (%), and P_c is capillary pressure (psi) corresponding to the apex of a hyperbolic log-log mercury injection plot. This equation for K_{air} has a standard deviation of 1.96×. Swanson also showed a similar relationship for brine permeability (md) at 1000 psi effective stress. This relationship was based on 56 clean sandstone and carbonate samples:

$$K_{brine} = 355\ (S_{HG}/P_c)_{apex}^{2.005} \quad (3)$$

which had an improved standard deviation of 1.67×. The advantage of using stressed liquid permeability is that overburden pressure and the gas slippage effect are taken into account. Swanson (1981) showed the relationship between stressed brine permeability and unstressed air permeability to be

$$K_{brine} = 0.292K_{air}^{1.186}. \quad (4)$$

Swanson (1981) also developed a nomograph based on equation 3, which uses the apex of the hyperbola of a log-log plot such as Figure 2. This nomograph permits direct estimation of brine permeability from mercury injection data.

Swanson (1981) showed that the apex was the same for core plug data and simulated drill cuttings (i.e., crushed rock from sample adjacent to the plug). This suggests that useful mercury injection data might be obtained from drill cuttings. Other workers also have expressed the opinion that useful mercury injection tests could be run on drill cuttings (Purcell, 1949; Ghosh et al., 1987).

Katz and Thompson (1986, 1987) reported the following relationship:

$$K = 1/226\ (l_c^2)\ (\sigma/\sigma_o) \quad (5)$$

where K = air permeability (md), l_c = characteristic pore size (i.e., the calculated pore size {μm} for threshold pressure at which mercury forms a connected pathway through the sample), and σ/σ_o = ratio of rock conductivity to conductivity of formation water.

This equation follows percolation theory arguments (e.g., Ambegaokar et al., 1971), which are applicable to systems characterized by a broad distribution of conductances with only short-range correlations. Seeburger and Nur (1984) showed that the pore spaces of many reservoir rocks have a random, broad distribution of pore sizes, which suggests that transport through pores must be understood in terms of a broad distribution of local conductances (Katz and Thompson, 1987). Equation 5 is applicable to sandstones and carbonates and appears to provide a good estimate of permeability (Thompson et al., 1987). This approach, however, requires a rock sample, laboratory measurement of threshold pressure, and measurement of rock and formation water conductivity.

Yuan and Swanson (1989) used a method of rate-controlled mercury porosimetry in which the injection rate is kept constant and the mercury pressure is monitored. Fluctuations in the mercury meniscus may occur because of varying degrees of constriction along the flow path. This enabled the researchers to resolve the

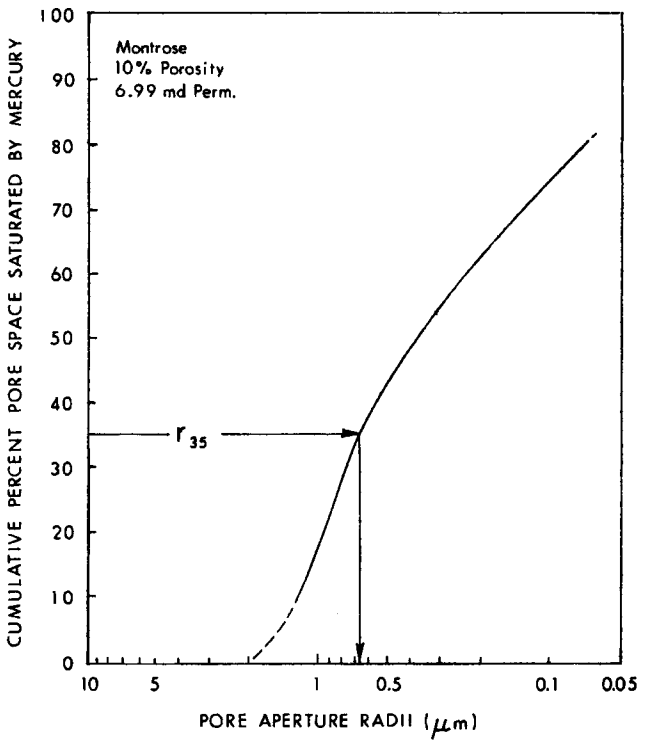

Figure 3—A semilog mercury injection plot with pore size plotted on the logarithmic axis.

pore space of a rock into pore bodies and pore throats. This technique appears promising for improving our understanding of pore geometry.

H. D. Winland (Amoco Production Company), who was interested in sealing potential, developed an empirical relationship among porosity, air permeability, and the pore aperture corresponding to a mercury saturation of 35% (r_{35}) for a mixed suite of sandstones and carbonates. Winland ran regressions for other percentiles (30, 40, and 50), but the best correlation (highest R) was the 35th percentile. No explanation was given for why the 35th percentile gave the best correlation. His data set included 82 samples (56 sandstone and 26 carbonate) with low permeabilities that were corrected for gas slippage and 240 other samples with uncorrected permeabilities. The Winland equation was used and published by Kolodzie (1980):

$$\text{Log } r_{35} = 0.732 + 0.588 \text{ Log } K_{air} - 0.864 \text{ Log } \emptyset \qquad (6)$$

where r_{35} is the pore aperture radius corresponding to the 35th percentile, K_{air} is uncorrected air permeability (md), and Ø is porosity (%).

Hartmann and Coalson (1990) correlated Winland's r_{35} values with pore type and reservoir quality. Winland favored plotting cumulative percent mercury saturation versus pore aperture radii on semilog paper, putting pore aperture radii on the log scale (Figure 3).

Winland also showed, through several field examples, that r_{35} could be used to delineate commercial hydrocarbon accumulations of stratigraphic traps. One of Winland's examples was the Terry Sandstone at Spindle Field, Colorado. Pittman (1989), using some of the same cored wells as Winland, showed that the net feet of sandstone having an r_{35} greater than 0.5 μm was useful for delineating the trap. Updip dry holes have no net sandstone with an r_{35} >0.5 μm; whereas, a good well in the field has 39 ft (11.9 m) of net sandstone with an r_{35} >0.5 μm.

PROCEDURE

Two hundred and two porosity and uncorrected air permeability analyses were available in the Amoco Research Center files on plugs that had also been used for mercury injection tests of sandstones from 14 formations. The porosities and permeabilities of the data set ranged from 3.3 to 28.0% and 0.05 to 998 md, respectively. These formations, which range in age from Ordovician to Tertiary, include Simpson, Delaware, Tensleep, Nugget, Cotton Valley, Muddy, Mesaverde, Terry, First Wall Creek, Second Wall Creek, Frontier, Montrose, Vicksburg, and Frio sandstones. Lithologically, these sandstones include sublitharenites, subarkoses, and quartz arenites in a modified Dott classification (Pettijohn et al., 1987). Argillaceous sandstones, clean permeable sandstones, and clean but tightly cemented sandstones are represented. The size of the sample suite coupled with the wide range in porosity and permeability, the diverse composition, and the variable texture of the sandstones suggests this should be a representative sample set for reservoir sandstones.

The threshold pressure and displacement pressure were determined graphically from the mercury injection curves, and the corresponding pore aperture radii were calculated using equation 1. The apex was determined graphically for each mercury injection curve by plotting mercury saturation pressure divided by mercury saturation on the y axis against mercury saturation on the x axis (Figure 4). Six of the 202 samples were nonhyperbolic and lacked an apex. Pore aperture radii corresponding to the 10th, 15th, 20th, 25th, 30th, 35th, 40th, 45th, 50th, 55th, 60th, 65th, 70th, and 75th percentiles of mercury saturation were also determined. A Statistical Analysis System (SAS) multiple regression program was used to establish various empirical relationships.

RESULTS

The graphical expression of the threshold pressure (Katz and Thompson, 1986), which is the inflection point of the curve, was determined for all mercury injection curves. For some samples, the inflection point was vague and difficult to determine. Using the radius

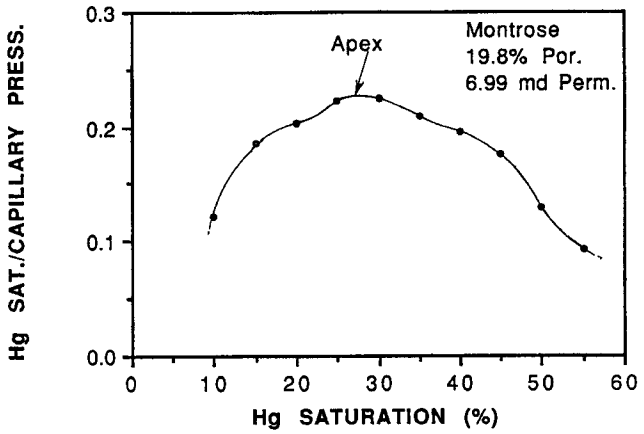

Figure 4—A plot of Hg saturation/capillary pressure versus Hg saturation, as a means of determining the apex of Thomeer's (1960) hyperbola. This is a more accurate method than the one depicted on Figure 2.

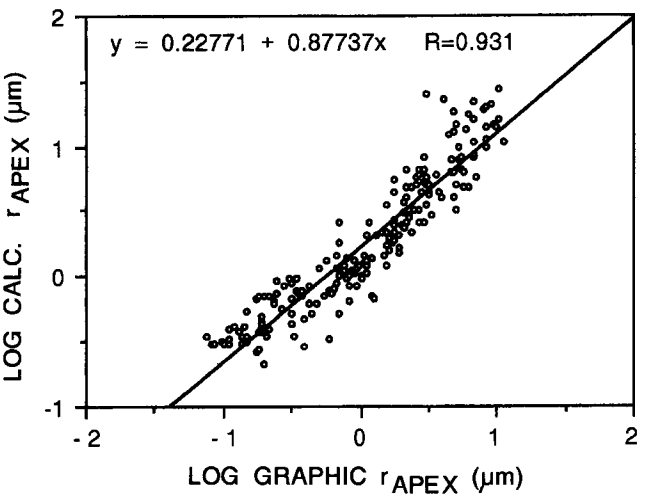

Figure 5—Plot of calculated pore aperture corresponding to the apex (equation 9) versus pore aperture of graphically derived apex (Figure 4).

of the pore aperture corresponding to the threshold pressure (r_{thresh} in μm) as the dependent variable in a multiple regression involving uncorrected air permeability (K in md), and porosity (Ø in %) yielded:

$$\text{Log } r_{thresh} = 0.137 + 0.479 \text{ Log } K - 0.143 \text{ Log } Ø. \quad (7)$$

This equation has a correlation coefficient of 0.900.

A relationship among the pore size corresponding to Schowalter's (1979) displacement pressure (r_{Pd} in μm), uncorrected air permeability (K in md), and porosity (Ø in %), was established by a multiple regression with log r_{Pd} as the dependent variable:

$$\text{Log } r_{Pd} = 0.459 + 0.500 \text{ Log } K - 0.385 \text{ Log } Ø. \quad (8)$$

This equation has a correlation coefficient of 0.901.

Based on a multiple regression with log r_{apex} as the dependent variable, the relationship among the pore size corresponding to the apex (r_{apex} in μm), uncorrected air permeability (K in md), and porosity (Ø in %) is

$$\text{Log } r_{apex} = -0.117 + 0.475 \text{ Log K} - 0.099 \text{ Log } Ø. \quad (9)$$

This equation yields a correlation coefficient of 0.919. The porosity term is not statistically significant in this equation. A regression excluding porosity as a variable also has an R of 0.919 and yields:

$$\text{Log } r_{apex} = -0.226 + 0.466 \text{ Log } K \quad (10)$$

where r_{apex} is in micrometers and K is uncorrected air permeability in millidarcys.

A graph of log r_{apex} calculated from equation 9 plotted against graphically determined r_{apex} (Figure 4) is shown in Figure 5. This plot has a correlation coefficient of 0.931. The mean apex for the 196 sandstones had a mercury saturation of 36%.

Winland's approach of using multiple regression analysis to develop an empirical equation for calculating the pore throat that corresponds to the 35th percentile was extended to a spread of mercury saturation percentiles (Table 1). For the lower percentiles of mercury saturation (10–35), the porosity term is not statistically significant and the pore aperture sizes could be predicted equally well using only permeability in the regression to develop an equation. The porosity term is statistically significant for the higher percentiles of mercury saturation (40–75). The reason for this is unknown. For simplicity, however, all the empirical equations in Table 1 include a porosity term. In Table 1, note that the correlation coefficient, R, decreases at increasingly higher percentiles. One can construct a partial pore aperture size distribution curve from the equations in Table 1, recognizing that the accuracy would diminish above the 55th percentile. For most sandstones, this would cover the important part of the curve. Regressions for pore apertures corresponding to mercury saturation percentiles from 10 to 55% had R values above 0.900. Figure 6 shows measured (via mercury injection) and calculated (equations, Table 1) pore aperture radius distribution curves for the same sample.

Using permeability as the dependent variable yielded the following empirical relationships:

$$\text{(a) Log } K = -0.861 + 1.185 \text{ Log } Ø + 1.627 \text{ Log } r_{apex} \quad (11)$$

with an R of 0.928. In this equation, K is uncorrected air permeability (md), Ø is porosity (%), and r_{apex} is the pore radius corresponding to the apex (μm).

$$\text{(b) Log } K = -1.221 + 1.415 \text{ Log } Ø + 1.512 \text{ Log } r_{25} \quad (12)$$

Table 1. Empirical Equations for Determining Pore Aperture Radii (μm) Corresponding to Various Mercury Saturation Percentiles

Equations	Correlation Coefficient
$\text{Log } r_{10} = 0.459 + 0.500 \text{ Log K} - 0.385 \text{ Log } Ø^*$	0.901
$\text{Log } r_{15} = 0.333 + 0.509 \text{ Log K} - 0.344 \text{ Log } Ø^*$	0.919
$\text{Log } r_{20} = 0.218 + 0.519 \text{ Log K} - 0.303 \text{ Log } Ø^*$	0.926
$\text{Log } r_{25} = 0.204 + 0.531 \text{ Log K} - 0.350 \text{ Log } Ø^*$	0.926
$\text{Log } r_{30} = 0.215 + 0.547 \text{ Log K} - 0.420 \text{ Log } Ø^*$	0.923
$\text{Log } r_{35} = 0.255 + 0.565 \text{ Log K} - 0.523 \text{ Log } Ø^*$	0.918
$\text{Log } r_{40} = 0.360 + 0.582 \text{ Log K} - 0.680 \text{ Log } Ø$	0.918
$\text{Log } r_{45} = 0.609 + 0.608 \text{ Log K} - 0.974 \text{ Log } Ø$	0.913
$\text{Log } r_{50} = 0.778 + 0.626 \text{ Log K} - 1.205 \text{ Log } Ø$	0.908
$\text{Log } r_{55} = 0.948 + 0.632 \text{ Log K} - 1.426 \text{ Log } Ø$	0.900
$\text{Log } r_{60} = 1.096 + 0.648 \text{ Log K} - 1.666 \text{ Log } Ø$	0.893
$\text{Log } r_{65} = 1.372 + 0.643 \text{ Log K} - 1.979 \text{ Log } Ø$	0.876
$\text{Log } r_{70} = 1.664 + 0.627 \text{ Log K} - 2.314 \text{ Log } Ø$	0.862
$\text{Log } r_{75} = 1.880 + 0.609 \text{ Log K} - 2.626 \text{ Log } Ø$	0.820

*Ø is statistically insignificant. A regression excluding Ø yields essentially the same result. k = permeability (md) and Ø = porosity (%).

yielded the best correlation coefficient, an R of 0.939. For equation 12, K is uncorrected air permeability (md), Ø is porosity (%), and r_{25} is the pore aperture corresponding to the 25th percentile of saturation on a cumulative mercury injection plot.

DISCUSSION

Sediments deposited in an aqueous environment have an affinity for water and are water-wet. After oil becomes trapped in a reservoir, polar organic compounds may adhere to the rock surface and through time make the rock oil-wet or partially oil-wet. However, for the purposes of migration and entrapment of hydrocarbons, rocks are considered to be water-wet. Following generation and expulsion of hydrocarbons from a source rock, the hydrocarbons move through a carrier bed as a nonwetting phase displacing water. Eventually, the hydrocarbons reach a position where the capillary pressure exceeds the opposing buoyancy pressure generated by the hydrocarbon column, and the hydrocarbons are trapped.

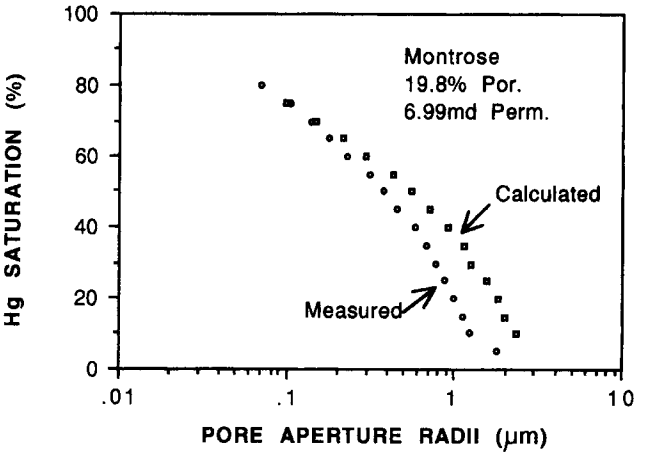

Figure 6—Comparison of measured (mercury injection) and calculated (equations, Table 1) pore aperture radius distribution curves for the same sample.

To evaluate migration and entrapment of hydrocarbons, it is necessary to identify the pore aperture size that would lead to entrapment. Ideally, this would be the threshold pressure, as measured in the laboratory by Katz and Thompson (1987), at which the mercury provides an interconnecting thread across the core plug to establish electrical conductivity. This approach, however, precludes the use of existing mercury injection tests. If porosity and permeability values from a core analysis are available, the pore aperture size corresponding to the displacement pressure can be predicted using equation 8. The threshold pressure as defined by Katz and Thompson (1986, 1987), would be more accurate than the displacement pressure as defined by Schowalter (1979). However, the graphical determination of threshold pressure, which is required for working with existing "old" data, is inaccurate, and thus equation 7 does not appear to be an improvement over equation 8. Calculation of displacement pressure pore radii from porosity and permeability values has the advantage of providing data throughout the cored interval instead of being limited to results from sparse mercury injection tests.

Berg (1975) recognized the limitations of sparse mercury injection test data. He developed an empirical equation to estimate grain size from porosity and permeability and then determined pore aperture radii by incorporating grain size in another equation. He states that this method "gives only a crude approximation of dominant pore size for natural sandstones" (Berg, 1975, p. 947). The empirical equations developed in this paper are an improvement over the approach used by Berg because these equations do not require estimation of grain size.

The pore aperture corresponding to the apex of the hyperbola on a log-log mercury injection plot is of significance because it represents the pore apertures that

interconnect to form what Swanson (1981) referred to as an effective pore system that dominates flow. Six of the 202 samples (2.9%) were nonhyperbolic and lacked an apex. These six samples ranged in porosity and permeability from 8.8 to 20.0% and 0.09 to 3.0 md, respectively. The permeability, however, was typically low (mean = 1.14 md). All of these samples had mercury injection curves that yielded essentially straight or slightly concave-upward curves when plotted on a semilog plot (e.g., Figure 7). Note that this type of sample has no dominant modal pore aperture size class on the histogram (Figure 7). If a dominant class and corresponding apex exist, that class is probably in the <10% mercury saturation range. Samples with an apex have mercury injection curve shapes that are convex-upward through most of the curve on a semilog plot (e.g., Figure 8). The apex corresponds to the dominant pore aperture class on the histogram (Figure 8).

The mean mercury saturation for the apex of Amoco's 196 sandstones was 36%, which is very close to the 35% that Winland used to delineate hydrocarbon accumulations in stratigraphic traps. Perhaps Winland found the best correlation to be for r_{35} because that is where the average modal pore aperture occurs and where the pore network is developed to the point of serving as an effective pore system that dominates flow in the sense described by Swanson (1981), based on his studies involving injection of Wood's metal.

A limited test of the applicability of equation 9 for apex radii was made in two wells previously studied in the Terry Sandstone stratigraphic trap at Spindle Field (Pittman, 1989). Results showed a favorable comparison between equation 9 and H. D. Winland's r_{35} (equation 6). An updip dry hole had no net feet of sandstone having a pore aperture of >0.5 μm using both equations. The calculated mean pore aperture size was 0.314 μm for apex and 0.326 μm for r_{35}. A producing well had 40 and 39 net ft (12.2 and 11.9 m) of sandstone having a pore aperture >0.5 μm, respectively, using apex and r_{35} equations. The calculated mean aperture radius for this producing well was 0.741 μm for apex and 0.671 μm for r_{35}. Thus, both equations appear to serve equally well for distinguishing nonproductive from productive wells for this trap.

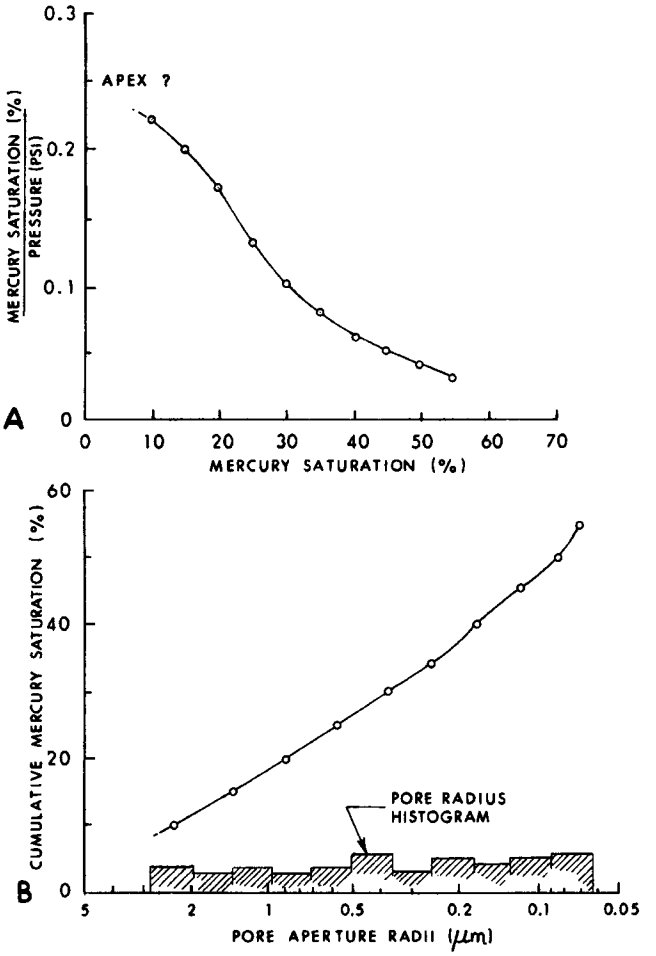

Figure 7—(A) Plot of mercury saturation versus mercury saturation divided by pressure, used to determine apex. If an apex exists for this sample, it must be at a saturation of <10%. (B) Semilog plot of pore aperture radii versus cumulative mercury saturation. Mercury injection data that do not have an apex yield cumulative curves that are essentially straight or slightly concave upward. The even distribution of pore radii on a histogram using $\log_2$ classes indicates the lack of a dominant modal class or classes. If a modal class exists, it is at a saturation of <10%; Wall Creek Sandstone, 13.8% porosity and 1.1 md permeability.

CONCLUSIONS

Porosity and uncorrected air permeability from routine core analysis can be used to estimate displacement pressure for use in the equations presented by Schowalter (1979), and to estimate the pore aperture size of the apex for use in delineating traps in a manner similar to the way r_{35} has been used.

Among 196 sandstone samples from 14 formations, the mean apex of log-log mercury injection plots was at a mercury saturation of 36%. The empirically derived relationships among uncorrected air permeability (K in md), porosity (Ø in %), and the pore aperture radius (μm) corresponding to the displacement pressure and apex, respectively, can be expressed as

$$\text{Log } r_{Pd} = 0.459 + 0.500 \text{ Log } K - 0.385 \text{ Log } Ø$$

and

$$\text{Log } r_{apex} = -0.117 + 0.475 \text{ Log } K - 0.099 \text{ Log } Ø.$$

Because these equations are based on uncorrected

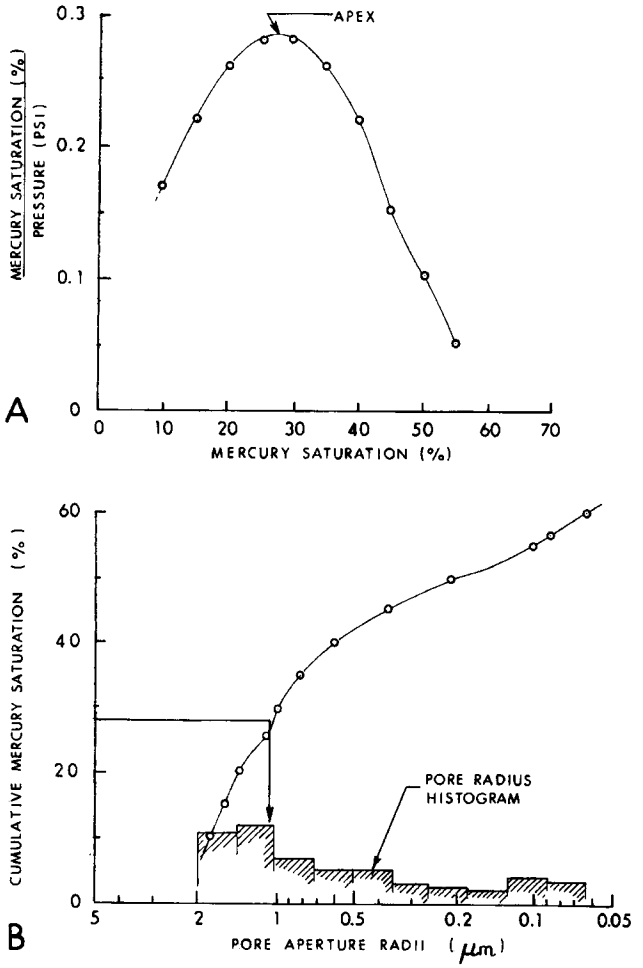

Figure 8—(A) Plot of mercury saturation versus mercury saturation divided by pressure, showing an apex at a saturation of 28%. (B) Semilog plot of pore aperture radii versus cumulative mercury saturation. The corresponding histogram (log_2 classes) has a modal pore aperture class between 1.41 and 1.0 μm and a weak secondary modal class from 0.125 to 0.088 μm. The coarser mode corresponds to the apex, which is where the pores occur that are capable of dominating flow; Terry Sandstone, 16.4% porosity and 1.8 md permeability.

air permeabilities, the use of corrected permeability values, which would be smaller, would produce a misleadingly smaller pore-aperture-size calculation.

The empirically derived equations of Table 1 correspond to mercury saturations from 10 to 75%, and permit the construction of a calculated pore-aperture-radius distribution curve that is based on porosity and uncorrected air permeability.

REFERENCES CITED

Ambegaokar, V., B. I. Halperin, and J. S. Langer, 1971, Hopping conductivity in disordered systems: Physical Review B, v. 4, p. 2612–2620.

Berg, R. R., 1975, Capillary pressure in stratigraphic traps: AAPG Bulletin, v. 59, p. 939–956.

Dullien, F. A. L., 1981, Wood's metal porosimetry and its relation to mercury porosimetry: Powder Technology, v. 29, p. 109–116.

Dullien, F. A. L., and G. K. Dhawan, 1974, Characterization of pore structure by a combination of quantitative photomicrography and mercury porosimetry: Journal of Colloid and Interface Science, v. 47, p. 337–349.

Dullien, F. A. L., and G. K. Dhawan, 1975, Bivariate pore-size distributions of some sandstones: Journal of Colloid and Interface Science, v. 53, p. 129–135.

Ghosh, S. K., S. F. Urschel, and G. M. Friedman, 1987, Substitution of simulated well-cuttings for core plugs in the petrophysical analysis of dolostones: Permian San Andres Formation, Texas: Carbonates and Evaporites, v. 2, p. 95–100.

Hartmann, D. J., and E. B. Coalson, 1990, Evaluation of the Morrow Sandstone in Sorrento Field, Cheyenne County, Colorado, *in* S. A. Sonnenberg, L. T. Shannon, K. Rader, W. F. Von Drehle, and G. W. Martin, eds., Morrow Sandstones of Southeast Colorado and Adjacent Areas, The Rocky Mountain Association of Geologists, Denver, Colorado, p. 91–100.

Katz, A. J., and A. H. Thompson, 1986, Quantitative prediction of permeability in porous rock: Physical Review B, v. 34, p. 8179–8181.

Katz, A. J., and A. H. Thompson, 1987, Prediction of rock electrical conductivity from mercury injection measurements: Journal of Geophysical Research, v. 92, p. 599–607.

Kolodzie, S., Jr., 1980, Analysis of pore throat size and use of the Waxman-Smits equation to determine OOIP in Spindle Field, Colorado: Society of Petroleum Engineers, 55th Annual Fall Technical Conference, Paper SPE-9382, 10 p.

Pettijohn, F. J., P. E. Potter, and R. Siever, 1987, Sand and sandstones, 2d ed., New York, Springer-Verlag, 553 p.

Pittman, E. D., 1989, Nature of the Terry Sandstone reservoir, Spindle Field, Colorado, *in* E. B. Coalson, ed., Petrogenesis and Petrophysics of Selected Sandstone Reservoirs of the Rocky Mountain Region, Rocky Mountain Association of Geologists, Denver, Colorado, p. 245–254.

Purcell, W. R., 1949, Capillary pressures—their measurement using mercury and the calculation of permeability therefrom: American Institute of Mechanical Engineers, Petroleum Transactions, Feb., p. 39–48.

Robinson, R. B., 1966, Classification of reservoir rocks by surface texture: AAPG Bulletin, v. 50, p. 547–559.

Schowalter, T. T., 1979, Mechanics of secondary hydrocarbon migration and entrapment: AAPG Bulletin, v. 63, p. 723–760.

Seeburger, D. A., and A. Nur, 1984, A pore space model for rock permeability and bulk modulus: Journal Geophysical Research, v. 89, no. B1, p. 527–536.

Smith, D. A., 1966, Theoretical considerations of sealing and nonsealing faults: AAPG Bulletin, v. 50, p. 363–374.

Swanson, B. F., 1977, Visualizing pores and non-wetting phase in porous rocks: Society of Petroleum Engineers, Annual Fall Technical Conference, SPE Paper 6857, 10 p.

Swanson, B. F., 1981, A simple correlation between permeabilities and mercury capillary pressures: Journal of Petroleum Technology, Dec., p. 2488–2504.

Thomeer, J. H. M., 1960, Introduction of a pore geometrical factor defined by the capillary pressure curve: Journal Petroleum Technology, Mar., p. 73–77.

Thompson, A. H., A. J. Katz, and R. A. Raschke, 1987, Estimation of absolute permeability from capillary pressure measurements: Society of Petroleum Engineers, 62nd Annual Technical Conference, Paper SPE-16794, p. 475–481.

Van Brakel, J., S. Modry, and M. Svata, 1981, Mercury porosimetry: state of the art: Powder Technology, v. 29, p. 1–12.

Washburn, E. W., 1921, Note on a method of determining the distribution of pore sizes in a porous material: Proceedings of the National Academy of Science, v. 7, p. 115–116.

Yuan, H. H., and B. F. Swanson, 1989, Resolving pore-space characteristics by rate-controlled porosimetry: SPE Formation Evaluation, March, p. 17–24.